www.ietdl.org

Published in IET Communications
Received on 26th January 2013
Revised on 19th March 2013
Accepted on 18th April 2013
doi: 10.1049/iet-com.2012.0819

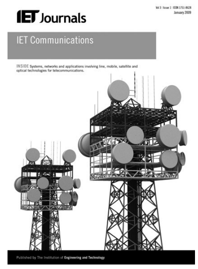

ISSN 1751-8628

Maximum Euclidean distance network coded modulation for asymmetric decode-and-forward two-way relaying

Wei Chen[1], Zhigang Cao[1], Lajos Hanzo[2]
[1]Department of Electronic Engineering, Tsinghua University, Beijing, People's Republic of China
[2]School of Electronics and Computer Science, University of Southampton, Southampton, UK
E-mail: lh@ecs.soton.ac.uk

Abstract: Network coding (NC) compresses two traffic flows with the aid of low-complexity algebraic operations, hence holds the potential of significantly improving both the efficiency of wireless two-way relaying, where each receiver is collocated with a transmitter and hence has prior knowledge of the message intended for the distant receiver. In this contribution, network coded modulation (NCM) is proposed for jointly performing NC and modulation. As in classic coded modulation, the Euclidean distance between the symbols is maximised, hence the symbol error probability is minimised. Specifically, the authors first propose set-partitioning-based NCM as an universal concept which can be combined with arbitrary constellations. Then the authors conceive practical phase-shift keying/quadrature amplitude modulation (PSK/QAM) NCM schemes, referred to as network coded PSK/QAM, based on modulo addition of the normalised phase/amplitude. To achieve a spatial diversity gain at a low complexity, a NC oriented maximum ratio combining scheme is proposed for combining the network coded signal and the original signal of the source. An adaptive NCM is also proposed to maximise the throughput while guaranteeing a target BEP. Both theoretical performance analysis and simulations demonstrate that the proposed NCM can achieve at least 3 dB signal-to-noise ratio gain and two times diversity gain.

1 Introduction

Network coding (NC) has emerged as a promising solution for future communication networks. The underlying core idea behind NC is the linear combination and compression of various traffic flows with the aid of algebraic operations at intermediate nodes, such as routers or relay stations. These network coded flows will be decoded at their destination nodes (DNs) by jointly processing multiple input flows arriving from different paths and/or by exploiting some prior knowledge. This ingenious methodology allows a multicasting network to approach its maximum-flow capacity bound [1] and hence to support high-speed multimedia applications. By exploiting the broadcast nature of wireless downlink (DL) environments, NC may also attain a substantial power and bandwidth efficiency gain in unicast wireless transmissions.

In the past decade, the theory and application of NC has attracted extensive investigations. The initial design objective was that of approaching the maximum-flow capacity bound of multicasting wired networks [1]. In an effort to formulate its unified theory, linear space-based and algebraic frameworks were proposed for single-source multicasting described by a general graph model [2, 3]. In contrast to wired networks, where NC relies on the global network topology, wireless networks are capable of flexibly applying NC for achieving substantial throughput gains for unicast flows. Of particular practical interest is the two-way relay-aided (TWR) sub-network topology, which relies on bi-directional/duplex relaying. To the best of our knowledge, Wu *et al.* [4] was the first NC-contribution on the practical subject of simultaneous information exchange between two unicast flows. Explicitly, the relay node (RN) computes the XOR of the two bits received from two distant nodes, and then broadcasts the XORed output bits, which can be decoded at a node by simply XORing the received bit with the bit which was originally transmitted from this node. Assuming the transmission of unbiased random bits, a 50% potential energy and bandwidth reduction may be achieved at the relay. To broaden the application of wireless NC, Katti *et al.* [5] considered another related sub-network topology, which was referred to as *X*-relaying.

Motivated by its dramatic gain, wireless NC has been extensively studied throughout the past decade. In particular, wireless NC can be categorised into two scenarios, namely the three-timeslot TWR, where the two source nodes (SNs) transmit in two different timeslots to avoid the mutual interference [4, 5], and the two-timeslot TWR, where both of the two sources transmit simultaneously, hence superimposing the two signals in air. The two-timeslot TWR was studied by Zhang *et al.* [6] and Popovski and Yomo. [6, 7], who proposed physical layer NC, also referred to as amplify-and-forward bi-directional

relaying, where the relay forwards a noisy version of the superimposed signal. To avoid forwarding the noise contribution, Koike-Akino *et al.* [8] proposed a denoise-and-forward protocol for two-timeslot TWR. By contrast, the three-timeslot TWR, also known as decode-and-forward (DF) TWR, results in 30% bandwidth efficiency loss compared to the two-timeslot TWR. However, it holds the promise of achieving higher diversity gain, broader applications and higher energy efficiency of RN, which will be realised in this paper. For three-timeslot TWR, it is critical to design NC of DL broadcast phase. In the symmetric case, where the rates of bi-directional flows are the same, the relay may simply calculate the bit-by-bit
Q1 XOR of each pair of bits and then maps the resultant NC bits to the transmitted symbols. However, asymmetric TWR is more practical, since the two-way traffic flows may have different symbol rates. Furthermore, the different link qualities and BER requirements of the two links may result in different channel coding rates and modulation constellations. In these asymmetric scenarios it is suboptimal to use conventional bit-level NC, such as the separate XOR addition and successive modulation. Hence, the efficient mapping of bits to symbols in the DL broadcast phase of three-timeslot TWR has been extensively studied [9–19]. The DL capacity of asymmetric DF-TWR was investigated in [9, 10]. More practically, NC was jointly designed with superposition coding [11], with physical layer coding [12], lattice coding [13] and with symbol level coding [14] to improve the asymmetric TWR. Most recently, the joint design of NC and modulation, which was also referred to as network coded modulation (NCM), has been investigated in [15–19], whereas a DF-based NC scheme was proposed in [20], where the bit-to-symbol mapping was optimised using a numerical search. Furthermore, a symbol-based physical-layer NC arrangement was proposed for a two-way relay channel in [21].

Against this background, we proposed a maximum-Euclidean-distance (ED) NCM for asymmetric DF-TWR, which may also rely on maximum ratio combining (MRC) detection. More specifically, although the XOR/modulo addition of non-binary symbol indices is indeed invertible and hence has no decoding ambiguity [9], the ED of legitimate symbols is usually not maximised. Our novel contribution is that the ED of legitimate symbols is maximised by jointly designing of NC and modulation. For arbitrary constellations, universal NCM is proposed based on the classic set partitioning technique of Ungerboeck originally conceived for maximising the minimum ED of the symbols in Trellis coded modulation (TCM) designed for point-to-point channels [22]. We will demonstrate that for phase-shift keying/quadrature amplitude modulation (PSK/QAM), practical NCM can be realised by the strikingly low-complexity modulo addition of the normalised phase/amplitude. Each receiver then decodes a rotated/circularly shifted PSK/QAM constellation. Furthermore, a low-complexity NC oriented MRC method is desired for combining the independent fading links originating from the RN and SN at the DN. However, the conventional MRC cannot be involved for combining the network coded and the original source symbols received at the destination (DN), because the symbols carried by the NC signal and the original source symbols are entirely different. Motivated by this, we then further propose the NC-MRC philosophy so as to combine the NC signal and the overheard original source signal at the DN. It is demonstrated that by invoking the proposed MRC conceived for NCM, the three-timeslot TWR becomes capable of achieving a full cooperative diversity gain of 2, thereby efficiently combating deep fades, because the DN is allowed to overhear the signals received from a distant SN. By contrast, the diversity order of two-timeslot TWR is upper bounded by 1 because of the half-duplex constraint. Furthermore, NCM is applicable to the *X*-relaying topology [5, 19], whereas two-timeslot TWR is not, because the concurrent transmission of two sources will cause severe mutual interference at both destinations. In this case, neither of the two destinations may obtain the prior knowledge required for network decoding by listening to its nearby source. Finally, NCM has a higher energy efficiency than the two-timeslot TWR, because NCM maximises the minimum ED. Note that the RN carrying two-way traffic consumes more energy and hence it becomes the bottleneck in energy constrained networks. Hence, it is critical to increase the energy efficiency of the RN. Based on the above arguments it may be concluded that NCM holds the promise of a wealth of near future applications.

The rest of this paper is organised as follows. Section 2 presents our system model. Section 3 describes the proposed universal maximum-ED NCM-based on set partitioning, which is applicable for arbitrary constellations. Section 4 proposes a more practical network coded PSK/QAM regime and provides both its (symbol error rate) SER analysis as well as its MRC detection and adaptive formulation. Section 5 compared NCM with various existing TWR schemes to demonstrate its performance gain. Our concluding remarks and further research ideas are provided in Section 6.

2 System model

Consider a TWR network, where a common RN transmits to DNs DN_1 and DN_2, each having a prior knowledge of the message intended for the other. Fig. 1*a* shows a bidirectional relaying network, where DN_1 and DN_2 also act as source nodes SN_1 and SN_2. Fig. 1*b* shows an X-relaying network [5, 19], where DN_1 and DN_2 may decode the signals sent by their source nodes SN_1 and SN_2, respectively. [In practice, a destination, for example, DN_1 Q2
may fail to decode the signal from its neighbour source SN_1. In this case, NC cannot be adopted. Therefore NC for *X*-relaying is usually implemented in an opportunistic way

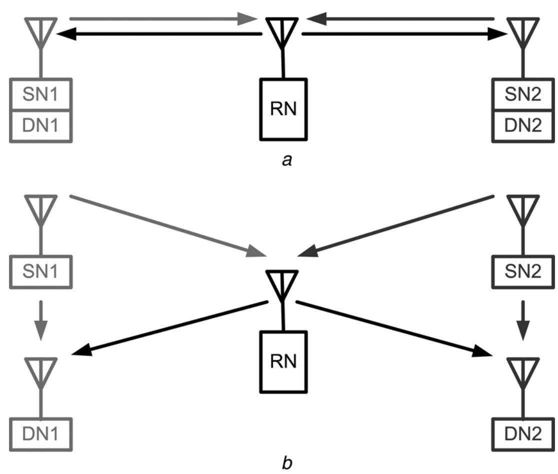

Fig. 1 *System model*

IET Commun., pp. 1–11
doi: 10.1049/iet-com.2012.0819

[5]. In this paper, we only focus on the scenario where destinations have successfully decoded the signal received from its neighbour sources.] Throughout this paper, we let $k = 3 - i$. Let W_i, $i = 1$, 2 denote the message of SN_k intended for DN_i. Thus, when we refer to DN_i, this receiver has the knowledge of W_k intended for DN_k. The data rate of the message W_i of SN_k is denoted by R_i. Without loss of generality, let us assume the message having the lower data rate of the two SNs to be W_1 and the message having the higher data rate to be W_2. Thus, we have $R_1 \leq R_2$ throughout this paper.

In TWR, the RN will transmit a single symbol, denoted by X, which simultaneously carries the messages to the two DNs. In each symbol duration T_s, $R_1 T_\mathrm{s}$ bits of W_1 and $R_2 T_\mathrm{s}$ bits of W_2 are jointly mapped to a symbol X chosen from a set $\mathcal{X}$, which is also referred to as the constellation. In practice, an integer number of bits is mapped to each symbol, that is, we have $R_i T_\mathrm{s} \in \mathbb{N}$. Conventionally, a constellation that carries $R_i T_\mathrm{s}$ bits/symbol must have $M_i = 2^{R_i T_\mathrm{s}}$ legitimate symbols. For $R_1 \leq R_2$, we have $(M_2/M_1) \in \mathbb{N}$. In this context, the equivalent baseband signal received at the coherent receiver of DN_i is represented by

$$Y_i = h_i X + Z_i \tag{1}$$

Note that SN_1 and SN_2 transmit in two different timeslots. In this case, DN_i is capable of overhearing the signal X_i^o transmitted by SN_k, which is presented by

$$Y_i^\mathrm{o} = g_i X_i^\mathrm{o} + Z_i^\mathrm{o} \tag{2}$$

In (1) and (2), Z_i and Z_i^o represent the additive white Gaussian noise (AWGN) at DN_i, with a noise variance of N_0, that is, we have $Z_i \sim \mathcal{CN}(0, N_0)$ and $Z_i^o \sim \mathcal{CN}(0, N_0)$. The fading channel coefficients spanning from the RN and SN_k to DN_i are denoted by h_i and g_i, respectively. RN_i are assumed to have the perfect channel state information (CSI) of h_i and g_i.

Assume that SN_k and RN have the same transmission power. Then the energy per symbol can be denoted by $E_\mathrm{s} := E|X|^2 = E\left|X_i^\mathrm{o}\right|^2$. Thus, the transmitter-side signal-to-noise ratio (SNR) is given by $\gamma = (2E_\mathrm{s}/N_0)$.

3 Set partitioning based-NCM

In this section, we introduce an universal NCM method based on adapting the classic set partitioning philosophy, which is referred to as SP-NCM. Given a modulation constellation, $\mathcal{X}$, our aim is to maximise the minimum distance of legitimate symbols for the receivers of both DN_1 and DN_2. To convey $R_2 T_\mathrm{s}$ bits per symbol, $\mathcal{X}$ must consist of M_2 symbols. Let $\mathcal{X}$ firstly be partitioned into (M_2/M_1) interlaced subsets, each consisting of M_1 symbols having the maximum possible symbol distances, that is, we have $\mathcal{X} = \bigcup_{n=0}^{M_2/M_1-1} \mathcal{X}^{(n)}$, $\mathcal{X}^{(n)} \cap \mathcal{X}^{(l)} = \emptyset$, for $n \neq l$. Let us label the symbols in the set $\mathcal{X}^{(n)}$ as $\{X^{(n)}[0], \ldots, X^{(n)}[M_1 - 1]\}$. Then the RN's transmitter will map both messages W_1 and W_2 into a single symbol X using the following SP-NCM algorithm (see Fig. 2).

Note that the legitimate symbols of message W_1 are always chosen from a subset $\mathcal{X}^{(n)}$, where the minimum ED is maximised. Embedding the message W_2 only determines which particular subsets to choose and hence affects how to select X within $\mathcal{X}^{(n)}$. As a result, the minimum ED of M_1 legitimate symbols of the message W_1 is still maximised even after embedding W_2. Furthermore, the constellation $\mathcal{X}$ consisting of only M_2 symbols is the minimum symbol set required for representing the message W_2. Accordingly, the minimum ED of the message W_2 is naturally maximised.

The receiver of DN_1 is capable of accurately inferring the subset $\mathcal{X}^{(n)}$ and the index m_2 by carrying out Steps 1 and 2 of the SP-NCM algorithm based on its prior knowledge of W_2. Then, the minimum distance criterion may be adopted for estimating $X[\hat{m}_1 + m_2 \bmod M_1]$ from $\mathcal{X}^{(n)}$, where the 'hat' ^ stands for the estimated value of a parameter. The decoding algorithm for $\hat{W}_1$ is summarised as shown in Fig. 3.

For DN_2, its receiver has to firstly estimate the transmitted symbol $X^{(\hat{n})}[m_1 + \hat{m}_2 \bmod M_1]$ from $\mathcal{X}$ using the minimum distance criterion. Then DN_2 can decode its desired message $\hat{W}_2$ based on its prior knowledge of m_1. The decoding algorithm of this receiver is presented as shown in Fig. 4.

As mentioned in the above, the legitimate symbols for the receiver of DN_1 always form a subset $\mathcal{X}^{(n)}$, in which the minimum ED has been maximised. Therefore the SER at the receiver of DN_1 is minimised. Unfortunately, the universal SER analysis of SP-NCM remains a challenge. To shed light on its performance, below a SER upper bound is presented. Note that based on the prior knowledge of W_k, there is a bijective mapping between W_i and the legitimate symbols of the receiver at DN_i. As a result, a symbol detection error occurs at DN_1 or DN_2 if and only if $X^{(n)}[\hat{m}_1]$ or $X[\hat{m}]$ is incorrectly estimated. Let the minimum ED of the symbols in $\mathcal{X}^{(n)}$ and $\mathcal{X}$ be denoted by

Algorithm 1

Step 1) Map W_2 to a symbol $X[m_2']$ in the original set $\mathcal{X}$.
Step 2) Find the unique subset $\mathcal{X}^{(n)}$ satisfying $X[m_2'] \in \mathcal{X}^{(n)}$ and the index m_2 satisfying $X^{(n)}[m_2] = X[m_2']$.
Step 3) Map W_1 to a symbol $X^{(n)}[m_1]$ in $\mathcal{X}^{(\backslash)}$.
Step 4) The transmitted symbol is given by $X = X^{(n)}[m_1 + m_2 \mod M_1]$.

Fig. 2 *Algorithm 1 set partitioning-based NCM*

Algorithm 2

Step 1) Map W_2 to a symbol $X[m_2']$ in the original set $\mathcal{X}$ given the prior knowledge of W_2.
Step 2) Find the unique subset $\mathcal{X}^{(n)}$ satisfying $X[m_2'] \in \mathcal{X}^{(n)}$ and the index m_2' satisfying $X^{(n)}[m_2] = X[m_2']$.
Step 3) Use the minimum distance criterion to estimate $X^{(n)}[\hat{m}_1] = \arg \min_{X^{(n)}[\hat{m}_1] \in \mathcal{X}^{(n)}} \left|X^{(n)}[\hat{m}_1] - h_1^{-1} Y_1\right|$.
Step 4) Decode the desired $\hat{W}_1$ from the estimated symbol $X^{(n)}[\hat{m}_1 - m_2 \mod M_1]$.

Fig. 3 *Algorithm 2 decoding algorithm for* $\hat{W}_1$

Algorithm 3

Step 1) Use the minimum distance criterion to estimate $X[\hat{m}] = \arg \min_{X[\hat{m}] \in \mathcal{X}} \left| X[\hat{m}] - h_2^{-1} Y_2 \right|$.

Step 2) Find the unique subset $\mathcal{X}^{(\hat{n})}$ satisfying $X[\hat{m}'] \in \mathcal{X}^{(\hat{n})}$ and the index $\hat{m}$ satisfying $X^{(\hat{n})}[\hat{m}] = X[\hat{m}']$.

Step 3) Map W_1 to a symbol $X^{(\hat{n})}[m_1]$ in $\mathcal{X}^{(\backslash)}$ given the prior knowledge of W_1.

Step 4) Decode the desired $\hat{W}_1$ from the estimated symbol $X^{(\hat{n})}[\hat{m} - m_1 \mod M_1]$.

Fig. 4 *Algorithm 3 decoding algorithm for $\hat{W}_2$*

$2d_1$ and $2d_2$, respectively. Based on Chapter 5.2 of [23], the SERs at DN_i can be upper bounded by

$$P_i < (M_i - 1) Q\left(\sqrt{\frac{|h_i|^2 d_i^2}{N_0/2}}\right)$$

The following example proposes SP-NCM using a PAM-like constellation, where the symbols are chosen from the real axis. Let us commence from a zero-mean M_1-ary PAM constellation subset $\mathcal{X}_0$ having a minimum ED of $2d_1$. Then $\mathcal{X}^{(n)}$ is obtained by the shifting operation as

$$\mathcal{X}^{(n)} = \mathcal{X}_0 + d_2\left[2n - \left(\frac{M_2}{M_1} - 1\right)\right],$$

$$n = 0, \ldots, \frac{M_2}{M_1} - 1, \quad \text{where} \quad d_2 \le \frac{M_1}{M_2} d_1$$

In this case, $\mathcal{X}^{(n)} \cap \mathcal{X}^{(l)} = \emptyset$, for $n \ne l$, and therefore, $\mathcal{X} = \bigcup_{n=0}^{M_2/M_1 - 1} \mathcal{X}^{(n)}$ has M_2 elements. From algebraic theory, we have $\mathcal{X} = \mathcal{X}_0 \oplus \mathcal{V}$, where $\oplus$ denotes the internal direct sum of two sets, and

$$\mathcal{V} = \left\{ d_2\left[2n - \left(\frac{M_2}{M_1} - 1\right)\right], \quad n = 0, \ldots, \frac{M_2}{M_1} - 1 \right\}$$

Note that $\mathcal{X}^{(n)}$ is a shifted version of a M_1-ary PAM with the minimum ED of $2d_1$. The SER of DN_1's receiver is

$$P_1 = \frac{2(M_1 - 1)}{M_1} Q\left(\sqrt{\frac{|h_1|^2 d_1^2}{N_0/2}}\right)$$

Proakis [24]. By observing that $d_2 \le (M_1/M_2) d_1$, we conclude that the minimum ED of $\mathcal{X}$ is $2d_2$. Since we have $\mathcal{X} \subseteq \mathbb{R}$, its SER is upper bounded by the SER of M_2-ary PAM having the minimum ED of $2d_2$, that is, we have

$$P_2 \le \frac{2(M_2 - 1)}{M_2} Q\left(\sqrt{\frac{|h_2|^2 d_2^2}{N_0/2}}\right)$$

Recalling that $\mathcal{X} = \mathcal{X}_0 \oplus \mathcal{V}$, we have $E\{X^2\} = E\{X_0^2\} + E\{V^2\}$, where $X_0 \in \mathcal{X}_0$ and $V \in \mathcal{V}$ are both uniformly distributed random variables with zero means. Therefore

$$E_s = \frac{M_1^2 - 1}{3} d_1^2 + \frac{M_1^{-2} M_2^2 - 1}{3} d_2^2$$

To provide further insights, let us consider DF analogue NC (DF-ANC), where $X = X_1 + X_2$ and X_i is chosen from a M_i-PAM constellation having a minimum symbol distance

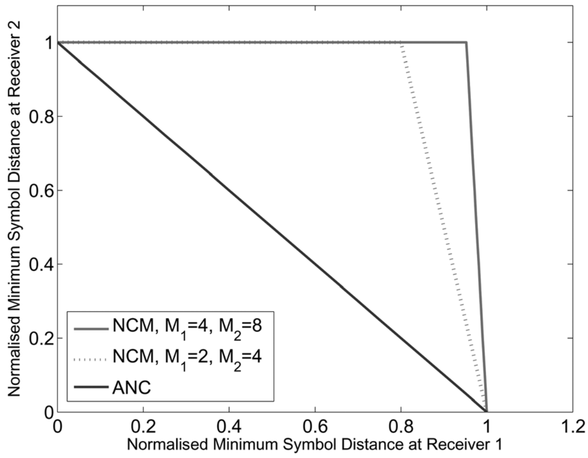

Fig. 5 *Comparison of the minimum distance of SP-NCM and DF-ANC*

$2d_i$. It may be readily seen that for DF-ANC, we have

$$E_s = \frac{M_1^2 - 1}{3} d_1^2 + \frac{M_2^2 - 1}{3} d_2^2$$

Fig. 5 compares the d_1^2 and d_2^2 tradeoffs of SP-NCM and DF-ANC. Clearly, given the same E_s, SP-NCM achieves a higher minimum ED and a lower SER.

4 Network coded PSK/QAM

In this section, we propose and analyse NCM designed for widely used PSK/QAM constellations, also referred to as NC-PSK/QAM, which may be interpreted as an instantiation of the unified SP-NCM concept. Specifically, maximum-ED NCM can be realised by the strikingly low-complexity modulo addition of the normalised phase/amplitude. Based on the NC-PSK/QAM design, a new NC oriented MRC is conceived, which is capable of combining the network coded signal received from the RN and the uncoded signal overheard from SN_k. An adaptive NCM is also proposed to maximise the throughput whereas guaranteeing a target BER.

4.1 NC-PSK and NC-QAM

In NC-PSK, the RN's transmitted symbol X is chosen from a M_2-ary PSK constellation through two steps. Firstly, $R_i T_s$ bits of the message W_i of SN_i will be mapped to a symbol chosen from a normalised M_i-ary PSK constellation having $M_i = 2^{R_i T_s}$ symbols, which are represented by

doi: 10.1049/iet-com.2012.0819

$\mathcal{X}_i = \{\cos\theta_i + j\sin\theta_i : \theta_i \in \Theta_i\}$, where we have

$$\Theta_i = \left\{0, \frac{2\pi}{M_i}, \ldots, \frac{2(M_i - 1)\pi}{M_i}\right\}$$

Any bit-to-symbol mapping methods, such as Gray coding or even classic TCM, can be adopted. Given the phase θ_1 and θ_2, the RN's transmitter generates an NC-PSK symbol given by

$$X = \sqrt{E_s}(\cos\theta + j\sin\theta) \tag{3}$$

where the symbol's phase is given by

$$\theta = \theta_1 + \theta_2 \bmod 2\pi \tag{4}$$

Note that Θ_i represents a finite group with respect to mod 2π addition, and the phase-set, Θ_1 is a subset of Θ_2 because of $(M_2/M_1) \in \mathbb{N}$. As a result, the group formed by the resultant phase is exactly Θ_2. It can be seen from (3) and (4) that the originally transmitted symbol of SN_k is rotated by an angle of θ_k at the RN, before its transmission to both DN_1 and DN_2.

Let us now turn our attention to the decoding algorithm of NC-PSK. To minimise the SER, the classic maximum a posteriori probability (MAP) detection rule is applied at both DN's receivers. Since the SN_i-data-dependent message W_k is also known at the receiver of DN_i, this receiver knows the rotation angel θ_k. Given the prior knowledge of θ_k, the receiver of DN_i will detect its desired symbol as

$$\begin{aligned}\hat{\theta}_i &= \arg\max_{\hat{\theta}_i \in \Theta_i} \Pr\Big\{h_i\sqrt{E_s}\big[\cos(\hat{\theta}_i + \theta_k) \\ &\quad + \mathrm{j}\sin(\hat{\theta}_i + \theta_k)\big]\Big| Y_i, h_i, \theta_k\Big\} \\ &= \arg\max_{\hat{\theta}_i \in \Theta_i} \left\| \arg(h_i^{-1} Y_i \exp \mathrm{j}\theta_k) - \hat{\theta}_i \right\|\end{aligned} \tag{5}$$

where arg(z) denotes the phase angle of a complex number z. Equation (5) shows the minimum distance criterion for NC-PSK. Given this formulation, we may infer the decision region of NC-PSK required for the decision variable $h_i^{-1}Y_i$ at the receiver of DN_i, as shown in Fig. 6, which can be obtained upon rotating the decision region of conventional

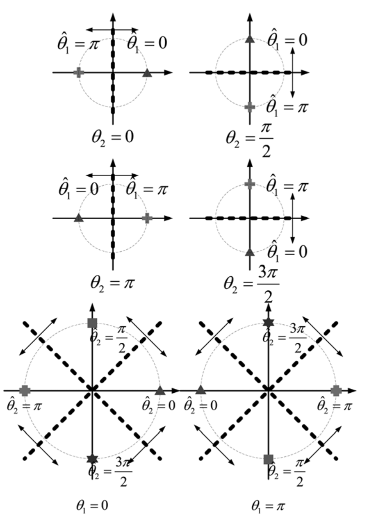

Fig. 6 *Decision regions for NC-PSK, $M_1 = 2$, $M_2 = 4$*

M_i-ary PSK by the above-mentioned angle θ_k. This implies that the detection complexity of NC-PSK is the same as that of classic PSK. Intuitively, the proposed NC-PSK may be inerpreted as a realisation of SP-NCM, when the constellation is PSK. Therefore the optimality of set partitioning guarantees the optimality of NC-PSK, in terms of both ED and SER. Moreover, when BPSK and QPSK are adopted, the constellation mapping of NC-PSK becomes equivalent to that of the scheme proposed in [20]. More particularly, Chen *et al.* [20] optimised the labelling for maximising the minimum distance within the constellation subset of MPSK, which was carried out with the aid of a numerical search. As stated by Chen *et al.* [20], this numerical search may impose a high complexity, when the constellations size is large. By contrast, we proposed a unified framework for NCM using set partitioning, which can be applied to arbitrary constellations. For practical constellations, such as MPSK, we exploited the constellation's algebraic structure for constructing the optimal NCM methods and found the associated closed-form solutions, rather than carrying out a numerical search. Furthermore, exploiting the beneficial algebraic structure of the constellations also allowed us to propose low-complexity decoding methods and to carry out the relevant SER analysis, which was not possible based on a numerical search.

Having conceived the transceiver scheme of NC-PSK, let us now study its SER performance. Recall from the above discussions that both the constellation and decision regions of NC-PSK are rotated versions of conventional M_i-ary PSK having a symbol energy of E_s. Intuitively, given the same symbol distances and decision rules, NC-PSK and conventional M_i-ary PSK should have the same SER. In particular, the average SER is equal to the SER conditioned on $\theta_i = 0$ and $\theta_k = 0$ for reasons of symmetry. As a result, we have

$$\begin{aligned}P_i &= \Pr\{\hat{\theta}_i \neq 0 | \theta_i = 0, \theta_k = 0\} \\ &= 2\Pr\left\{\left|\arg\left[\sqrt{E_s + \Re\mathrm{e}[Z_i]^2} + \mathrm{j}\Im\mathrm{m}[Z_i]\right]\right| \geq \frac{\pi}{M_i}\right\}\end{aligned}$$

From [24], we can arrive at the SER expression P_i at the receiver of DN_i as

$$P_i \simeq \left(1 + \mathcal{I}_{\{M_i > 2\}}\right) Q\left(\sqrt{\gamma_i}\sin\frac{\pi}{M_i}\right) \tag{6}$$

which is conditioned on the receiver-side SNR denoted by $\gamma_i = |h_i|^2\gamma$. Equation (6) implies the optimality of NC-PSK, which achieves the same SER at the receiver of the DN, as if the RN exclusively transmitted to a single receiver only. This SER property of NC-PSK is also recognised in parallel to the capacity property of NC in [9, 10], suggesting that both the $RN–DN_1$ and $RN–DN_2$ links are capable of approaching their own single-link capacity.

Let us now extend our attention to QAM, where NC-QAM is implemented in two steps per symbol duration. Note that the in-phase (I) and quadrature (Q) components of rectangular M-QAM may be regarded as a pair of $\sqrt{M}$-PAM signals [23]. As a result, in this work, we present NC-QAM as a set of two parallel NC-PAM schemes. First, R_iT_s bits of the message W_i will be mapped to a symbol from the set of M_i-ary PAM constellation

doi: 10.1049/iet-com.2012.0819

points, which is formulated as

$$\mathcal{X}_i = \left\{2\sqrt{M_i}\left(a_i^I + \mathrm{j}a_i^Q\right) - \left(\sqrt{M_i} - 1\right)(1+j): a_i^I, a_i^Q \in \mathcal{A}_i\right\},$$

$$\text{where} \quad \mathcal{A}_i = \left\{0, \frac{1}{\sqrt{M_i}}, \ldots, \frac{\sqrt{M_i}-1}{\sqrt{M_i}}\right\}$$

Given the normalised amplitudes $\left(a_1^I, a_1^Q\right)$ and $\left(a_2^I, a_2^Q\right)$, the RN's transmitter will generate the NC-QAM symbol as

$$X = d\left[2\sqrt{M_2}\left(a^I + \mathrm{j}a^Q\right) - \left(\sqrt{M_2} - 1\right)(1+j)\right] \quad (7)$$

where the normalised amplitude is given by

$$a^I = a_1^I + a_2^I \bmod 1 \quad (8)$$

$$a^Q = a_1^Q + a_2^Q \bmod 1 \quad (9)$$

and $d = \sqrt{\left((3E_\mathrm{s})/2(M_2-1)\right)}$ denotes half of the symbol distance in QAM, given an energy of E_s per symbol. When NC-QAM is adopted, the symbol to be transmitted to DN_k will be circularly shifted by an amplitude of $2\sqrt{M_2}\left(a_k^I + ja_k^Q\right)d$ at the RN.

Again, the receiver of DN_i knows $\left(a_k^I + \mathrm{j}a_k^Q\right)$ a priori and hence it will detect the symbol from a circularly shifted M_i-ary QAM constellation. Therefore both the detection methods and the SER analysis of conventional QAM can be borrowed for NC-QAM. The MAP detection method of NC-QAM at DN_i is formulated as follows

$$\begin{aligned}\hat{a}_i &= \arg\max_{\hat{a}_i^I, \hat{a}_i^Q \in \mathcal{A}_i} \Pr\Big\{h_i d\Big[2M_2\Big[\left(\hat{a}_i^I + a_k^I \bmod 1\right) \\ &\quad + \mathrm{j}\left(\hat{a}_i^Q + a_k^Q \bmod 1\right)\Big] - \left(\sqrt{M_2} - 1\right)(1+j)\Big]\Big| Y_i, h_i, a_k\Big\} \\ &= \arg\max_{\hat{a}_i^I, \hat{a}_i^Q \in \mathcal{A}_i} \Bigg\| \frac{h_i^{-1}Y_i + \left(\sqrt{M_2}-1\right)(1+j)d}{2d\sqrt{M_2}} \\ &\quad - a_k^I - \mathrm{j}a_k^Q + \mathcal{I}_{\left\{\hat{a}_i^I \geq 1 - a_k^I\right\}} + \mathrm{j}\mathcal{I}_{\left\{\hat{a}_i^Q \geq 1 - a_k^Q\right\}} - \hat{a}_i^I - j\hat{a}_i^Q \Bigg\|\end{aligned} \quad (10)$$

which is essentially the minimum distance criterion conceived for NC-QAM. Fig. 7 shows the decision region of an *I*/*Q* component of NC-QAM for the decision variable $h_i^{-1}Y_i$, which is a circularly shifted version of that of conventional QAM.

Next, let us derive the SER of NC-QAM. Intuitively, the SER of a circularly shifted M_i-ary QAM constellation is identical to that of the original M_i-ary QAM for the same minimum symbol distance. By recalling (7)–(9) and that $a_i^I, a_i^Q \in \mathcal{A}_i$, we have $d_1 = \left(\sqrt{M_2}/\sqrt{M_1}\right)d$ and $d_2 = d$. Let us insert d_1 and d_2 into

$$P_i = \frac{4\left(\sqrt{M_i}-1\right)}{\sqrt{M_i}} Q\left(\sqrt{\frac{|h_i|^2 d_i^2}{N_0/2}}\right)$$

and introduce the M_1 and M_2-dependent coefficient $\lambda_i = \left(1 - M_i^{-1}/1 - M_2^{-1}\right)$. We may thus arrive at the unified SER expressions of NC-QAM, given by

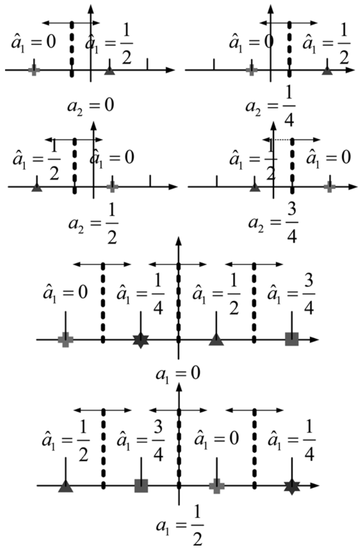

Fig. 7 *Decision regions for I/Q component of NC-QAM,* $\sqrt{M_1} = 2$, $\sqrt{M_2} = 4$

$$P_i = \frac{4\left(\sqrt{M_i}-1\right)}{\sqrt{M_i}} Q\left(\sqrt{\frac{1.5\lambda_i\gamma_i}{M_i - 1}}\right) \quad (11)$$

which is also conditioned on $\gamma_i = |h_i|^2\gamma$.

Note that $\lambda_2 = 1$. Accordingly, NC-QAM is capable of achieving a SER at the higher-rate receiver of DN_2 as if the RN transmitted exclusively to this single receiver only. For DN_1, however, the coefficient is $\lambda_1 \leq 1$, which implies imposing an SNR loss that remains constant across the entire SNR range. The reason for this SNR loss at the receiver of DN_1 can be stated as follows. As QAM is regarded as a pair of PAM, we may simply focus our discussion on the *I* component. Given a_2^I, the legitimate symbols at the receiver of DN_1 have a non-zero mean of

$$d\left[2\sqrt{M_2}\left(a_2^I \bmod \frac{1}{\sqrt{M_1}}\right) + 1 - \frac{\sqrt{M_2}}{\sqrt{M_1}}\right]$$

In contrast to the classic zero-mean $\sqrt{M_1}$–ary PAM, the DC bias of such a circularly shifted $\sqrt{M_1}$–ary PAM constellation will cost some extra energy, which therefore results in the above-mentioned SNR loss. Fortunately, the SNR loss of DN_1, λ_1, is an increasing function of M_2, but a deceasing function of M_1. Specifically, it is lower bounded by

$$\lambda_1 = \frac{1 - M_1^{-1}}{1 - M_2^{-1}} > 1 - \frac{1}{M_1} = \frac{3}{4}$$

In other words, the modest SNR loss imposed by NC-QAM will be < 1.25 dB. Furthermore, this lower bound also implies that the SNR loss becomes negligible, when M_1 is large. As a result, the proposed NC-QAM becomes capable of approximately maximising the EDs of the legitimate symbols at both DN_1 and DN_2. This implies the near-optimality of NC-QAM. Recall the example of

doi: 10.1049/iet-com.2012.0819

SP-NCM in Section 3, which can be reduced to NC-PAM for

$$d_1 = \frac{\sqrt{M_2}}{\sqrt{M_1}}\sqrt{\frac{3E_s}{2(M_2-1)}} \quad \text{and} \quad d_2 = \sqrt{\frac{3E_s}{M_2-1}}$$

Based on the set-partitioning argument, we may conclude that the ED of legitimate symbols in NC-QAM has been maximised.

4.2 Average SER of Rayleigh fading channels and NC-MRC

The TWR concept essentially relies on the wireless environment, since its broadcasting nature facilitates NC. However, the hostile fading effects may severely degrade the attainable transmission reliability. In this subsection, we conceive from the average SER analysis of NC-PSK/QAM in Rayleigh fading channels. We propose a low-complexity scheme for combining the NCM signal received from the RN and the original signal overheard from the SN so as to achieve a spatial diversity gain.

Recall that the above SER results of (6) and (11) represent the SER conditioned on a given receiver-side SNR of $\gamma_i = |h_i|^2\gamma$. Let us then rewrite the conditional SER $P_i(\gamma_i)$ as a function of γ_i. Intuitively, the average SER is then formulated as

$$\langle P_i \rangle = \int_0^\infty P_i(\gamma_i)\frac{1}{\bar{\gamma}_i}\exp\left(\frac{\gamma_i}{\bar{\gamma}_i}\right)\mathrm{d}\gamma_i$$

for Rayleigh fading channels, where the average receiver-side SNR is $\overline{\gamma_i} = |h_i|^2\gamma$. It is seen from (6) that the average SER of NC-PSK is identical to that of classic M_i-PSK. From Eq. (8.113) of [25], we have

$$\langle P_i \rangle_{\text{PSK}} = \frac{M_i - 1}{M_i}\left\{1 - \frac{M_i c_i(\bar{\gamma}_i)}{(M_i-1)\pi}\left[\frac{\pi}{2} + \tan^{-1}\left(c_i(\bar{\gamma}_i)\cot\frac{\pi}{M_i}\right)\right]\right\} \quad (12)$$

where

$$c_i(\bar{\gamma}_i) = \sqrt{\frac{\bar{\gamma}_i \sin^2(\pi/M_i)}{1 + \bar{\gamma}_i\sin^2(\pi/M_i)}}$$

For NC-QAM, however, one should take into account the coefficient λ_i. From Eq. (8.106) of [25] [For convenience, we use its high-SNR approximation throughout this paper.], the average SER of NC-QAM can then be formulated as

$$\langle P_i \rangle_{\text{QAM}} = \frac{2\left(\sqrt{M_i}-1\right)}{\sqrt{M_i}}\left(1 - \sqrt{\frac{1.5\lambda_i\bar{\gamma}_i}{M_i - 1 + 1.5\lambda_i\bar{\gamma}_i}}\right) \quad (13)$$

From (12) and (13), the diversity orders of both NC-PSK and NC-QAM are obtained as $\lim_{\bar{\gamma}_i\to\infty}\left(\log\langle P_i\rangle / \log\bar{\gamma}_i\right) = 1$. In other words, the average SER decreases slowly upon increasing the SNR, simply because of the effects of deep fading. To overcome this impediment, we combine the signals received from the independently fading paths so as to achieve some spatial diversity gain. In the topology considered, there are two independent paths, one arriving from the RN and the other from SN_k. In conventional one-way relaying, the DN may readily combine the two signals received from the SN and RN, because the signals transmitted by the RN are simply amplified versions of the SN's signals. When NC or NCM is employed at the RN, however, the NC signal and the original signal transmitted by the SN tend to be totally different. This renders the conventional MRC scheme inapplicable to TWR.

Fortunately, by carefully observing the relationship of the NC-PSK/QAM and the classic PSK/QAM, we may conceive a NC-MRC scheme for combining the NC signal received from the RN and the original signal overheard from SN_k. To do this, let us first derive the minimum distance criterion for NC-PSK/QAM from the MAP criterion. Let $X_i^{\text{o}}(W_i)$ and $X(W_1, W_2)$ represent the mapping from the messages W_i to the signals X_i^{o} and X. In this context

$$\hat{W}_i = \arg\max_{W_i} \Pr\left\{X_i^{\text{o}}(W_i), X(W_1, W_2) | Y_i^{\text{o}}, Y_i\right\} \quad (14)$$

$$= \arg\max_{W_i} \Pr\left\{Y_i^{\text{o}}, Y_i | X_i^{\text{o}}(W_i), X(W_1, W_2)\right\} \quad (15)$$

$$= \arg\max_{W_i} \Pr\left\{Y_i^{\text{o}}, Y_i | X_i^{\text{o}}(W_i), \Xi_k\left(X_i^{\text{o}}(W_i)\right)\right\} \quad (16)$$

where $\Xi_k(X_i^{\text{o}})$ represents a deterministic mapping. Specifically, we have $\Xi_k(X_i^{\text{o}}) = X_i^{\text{o}}\exp(-j\theta_k)$ for NC-PSK and (see equation at the bottom of the page)

for NC-QAM. Given this deterministic relationship between X_i^{o} and X, the conditional probability in (16) may be simplified to $\hat{W}_i = \arg\max_{W_i}\Pr\left\{Y_i, Y_i^{\text{o}} | X_i^{\text{o}}(W_i)\right\}$. Therefore the transmitted symbol $\hat{X}_i^{\text{o}}$ is estimated as

$$\hat{X}_i^{\text{o}} = \arg\max_{X_i^{\text{o}}} \Pr\left\{gX_i^{\text{o}} + Z_i^{\text{o}}, h_i\Xi_k(X_i^{\text{o}}) + Z_i | X_i^{\text{o}}\right\} \quad (17)$$

$$= \arg\min_{X_i^{\text{o}}} \left\|Y_i^{\text{o}} - gX_i^{\text{o}}\right\|^2 + \left\|Y_i - h_i\Xi_k\left(X_i^{\text{o}}\right)\right\|^2 \quad (18)$$

For NC-PSK, the above minimum distance decision criterion may be simplified to [In the following derivation, we shall also include the derivation of the conventional MRC scheme [24]. In particular,

$$\arg\min_x \|\boldsymbol{y} - \boldsymbol{h}x\|^2 = \arg\min_x |x|^2 - x\frac{(\boldsymbol{h}^*\boldsymbol{y})^*}{\|\boldsymbol{h}\|^2} - x^*\frac{\boldsymbol{h}^*\boldsymbol{y}}{\|\boldsymbol{h}\|^2}$$
$$= \arg\min_x \left\|\frac{\boldsymbol{h}^*}{\|\boldsymbol{h}\|^2\boldsymbol{y}} - x\right\|$$

$$\Xi_k(X_i^{\text{o}}) = d\left\{2\sqrt{M_2}\left[\left(\frac{\Re\mathrm{e}(X_i^{\text{o}}) + d_i\left(\sqrt{M_i}-1\right)}{2d_i\sqrt{M_i}} + a_k^I \bmod 1\right)\right.\right.$$
$$\left.\left. + \left[\mathrm{j}\left(\frac{\Im\mathrm{m}(X_i^{\text{o}}) + d_i\left(\sqrt{M_i}-1\right)}{2d_i\sqrt{M_i}} + a_k^Q \bmod 1\right) - \left(\sqrt{M_2}-1\right)(1+j)\right\}\right.$$

where * represents the conjugate complex operation. It is also worth noting that based on the above derivation the attainable SNR gain of MRC, which is $\|\boldsymbol{h}\|^2(E|x|^2/N_0/2)$.] becomes

$$\begin{aligned}\hat{\theta}_i &= \arg\min_{\hat{\theta}_i \in \Theta_i} \left\| Y_i^{\mathrm{o}} - g_i\sqrt{E_{\mathrm{s}}}\exp\left(-\mathrm{j}\hat{\theta}_i\right)\right\|^2 \\ &\quad + \left\| Y_i - h_i\sqrt{E_{\mathrm{s}}}\exp\left[-\mathrm{j}\left(\hat{\theta}_i + \theta_k\right)\right]\right\|^2 \\ &= \arg\min_{\hat{\theta}_i \in \Theta_i} \left\| Y_i^{\mathrm{o}} - g_i\sqrt{E_s}\exp\left(-\mathrm{j}\hat{\theta}_i\right)\right\|^2 \\ &\quad + \left\| Y_i \exp \mathrm{j}\theta_k - h_i\sqrt{E_s}\exp\left(-\mathrm{j}\hat{\theta}_i\right)\right\|^2 \\ &= \arg\min_{\hat{\theta}_i \in \Theta_i} \left\| \arg Y_{\mathrm{PSK}}^{\mathrm{MRC}} - \hat{\theta}_i \right\|\end{aligned}$$

where the NC-MRC's decision variable is given by

$$Y_{\mathrm{PSK}}^{\mathrm{MRC}} = g_i^* Y_i^{\mathrm{o}} + h_i^* Y_i \exp \mathrm{j}\theta_k \tag{19}$$

Equation (19) combines the original signal received from the SN and the appropriately rotated NC signal received from the RN, which carries the original symbol. Given the NC-MRC scheme's decision variable of $Y_{\mathrm{PSK}}^{\mathrm{MRC}}$, the decoding complexity is seen to be the same as that of classic M_i-ary PSK.

Observing that $E|Y_i \exp \mathrm{j}\theta_k|^2 = E_{\mathrm{s}}$, we arrive at the equivalent SNR of the NC-MRC decoder for NC-PSK given by $\gamma_i = (|h_i|^2 + |g_i|^2)\gamma$. In other words, the SNR is improved by a factor of $|g_i|^2\gamma$, which is an explicit benefit of NC-MRC. This also implies that the energy of the signal overheard from SN_k is fully exploited. In this case, the SER conditioned on the channel gains h_i and g_i is given by

$$P_i \simeq \left(1 + \mathcal{I}_{\{M_i > 2\}}\right) Q\left(\sqrt{\left(|h_i|^2 + |g_i|^2\right)\gamma}\sin\frac{\pi}{M_i}\right)$$

From Eq. (9.15) of [25], we arrive at the average SER of NC-PSK relying on MRC as follows

$$\begin{aligned}&\langle P_i \rangle_{\mathrm{PSK}}^{\mathrm{MRC}} \\ &= \frac{1}{\pi}\int_0^{((M_i-1)\pi/M_i)} \frac{\sin^4\phi}{\left(\sin^2\phi + \eta_i\overline{|h_i|^2}\bar{\gamma}\right)\left(\sin^2\phi + \eta_i\overline{|g_i|^2}\bar{\gamma}\right)}\mathrm{d}\phi\end{aligned} \tag{20}$$

where $\eta_i = \sin^2(\pi/M_i)$.

Next, let us simplify the minimum distance criterion of NC-QAM to that of MRC aided NC-QAM. For convenience, let us introduce the short-hand

$$g_i = g\sqrt{\frac{M_2 - 1}{M_i - 1}} = g\lambda_i^{-1/2}\sqrt{\frac{M_2}{M_i}}$$

Similarly, based on (18), we have

$$\hat{a}_i = \arg\min_{\hat{a}_i \in \mathcal{A}_i} \left\| Y_{\mathrm{QAM}}^{\mathrm{MRC}} - \hat{a}_i \right\| \tag{21}$$

where the NC-MRC's decision variable is given by (see (22)) where $\mu(\hat{a}_i, a_k) = \mathcal{I}_{\left\{\hat{a}_i^I \geq 1 - a_k^I\right\}} + j\mathcal{I}_{\left\{\hat{a}_i^Q \geq 1 - a_k^Q\right\}} - a_k^I - ja_k^Q$. Equation (22) combines the original signal received from the SN and the circularly shifted version of the NC signal received from the RN. The decoding complexity of the NC-MRC's output variable $Y_{\mathrm{QAM}}^{\mathrm{MRC}}$ is equal to that of M_i-ary QAM. Clearly, the equivalent SNR of the M_i-ary QAM decoder is $\gamma_i = \left(|h_i|^2 + \lambda_i^{-1}|g_i|^2\right)\gamma$. As a result, the SER conditioned on h_i and g_i is expressed as

$$P_i = \frac{4\left(\sqrt{M_i} - 1\right)}{\sqrt{M_i}} Q\left(\sqrt{\frac{1.5\left(\lambda_i|h_i|^2 + |g_i|^2\right)\gamma}{M_i - 1}}\right)$$

which shows that the energy of the overheard signal is fully exploited in order to bring about an additional SNR gain of $|g_i|^2\gamma$. From Eq. (9.15) of [25], the average SER of NC-QAM relying on NC-MRC may be formulated as

$$\begin{aligned}\langle P_i \rangle_{\mathrm{QAM}}^{\mathrm{MRC}} &= \frac{4\left(\sqrt{M_i} - 1\right)}{\pi\sqrt{M_i}} \\ &\quad \times \int_0^{(\pi/2)} \frac{\sin^4\phi}{\left(\sin^2\phi + \kappa_i\lambda_i\overline{|h_i|^2}\bar{\gamma}\right)\left(\sin^2\phi + \kappa_i\overline{|g_i|^2}\bar{\gamma}\right)}\mathrm{d}\phi\end{aligned} \tag{23}$$

where $\kappa_i = (1.5/(M_i - 1))$.

More importantly, (20) and (23) allow us to analyse the diversity gain of NC-MRC. In particular, it may be readily shown that

$$\lim_{\bar{\gamma}\to\infty} \frac{\log\langle P_i \rangle_{\mathrm{PSK}}^{\mathrm{MRC}}}{\log\bar{\gamma}} = \lim_{\bar{\gamma}_i\to\infty} \frac{\log\langle P_i \rangle_{\mathrm{QAM}}^{\mathrm{MRC}}}{\log\bar{\gamma}} = 2$$

that is, the diversity order of NC-PSK/QAM relying on NC-MRC is 2. Clearly, the proposed NC-MRC achieves the maximum diversity order of 2 by combining the RN's NC signal and the SN's signal arriving from two independently fading paths. It is worth noting that this cannot be achieved for two-timeslot TWR, where the two SNs transmit to the RN simultaneously. For the bi-directional relaying scenario of Fig. 1*a*, this is simply because of the half duplex constraint, which forbids for the DN to receive from the channel, when it transmits. For X-relaying shown in Fig. 1*b*, this is because the concurrent transmission of two SNs will inflict severe mutual interference upon the DN. By contrast, the three-timeslot TWR regime has a lower spectral efficiency, but it is capable of achieving a cooperative diversity gain of 2, which is highly desirable in a severely fading wireless environment.

$$Y_{\mathrm{QAM}}^{\mathrm{MRC}} = \frac{\sqrt{\lambda_i^{-1}}g^* Y_i^o + h_i^* Y_i - d(1+j)\left(|g_i|^2\sqrt{(M_2/\lambda_i M_i)} + |h_i|^2\right) + 2d\sqrt{M_2}|h_i|^2\mu\left(\hat{a}_i, a_k\right)}{2d\sqrt{M_2}\left(\lambda_i^{-1}|g_i|^2 + |h_i|^2\right)} + \frac{1}{2}(1+j) \tag{22}$$

IET Commun., pp. 1–11
doi: 10.1049/iet-com.2012.0819

4.3 Adaptive NCM

In this subsection, an adaptive NCM scheme is proposed for maximising the data rates of two-way links under certain BER constraints. Recalling the similarity of the SER formulas between NC-PSK/QAM and conventional PSK/QAM, we may conceive the adaptive NCM from conventional adaptive modulation [26, 27]. Conventional adaptive PSK will map the transmitter's data to a symbol from 2^n-ary PSK, when the receiver-side SNR is $\gamma_{\text{PSK}} \in \left[\gamma_{\text{PSK}}^{(n)}, \gamma_{\text{PSK}}^{(n+1)}\right]$, where $\gamma^{(n)\text{PSK}}, n = 1, 2 \ldots$ denotes the minimum SNR required for 2^n-ary PSK to meet the target BER. Since the SER expression (6) of NC-PSK is exactly the same as that of PSK, the modulation order M_i of the RN-DN$_i$ link can be chosen in the same way. In particular, we have $M_i = 2^n$ for $\gamma_i = |h_i|^2\gamma \in \left[\gamma_{\text{PSK}}^{(n)}, \gamma_{\text{PSK}}^{(n+1)}\right)$. When NC-MRC is adopted, the receiver side SNR is increased to $\gamma_i = (|h_i|^2 + |g_i|^2)\gamma$. In this case, however, SN$_k$ and RN should use the same M_i-PSK constellation so that DN$_i$ may efficiently combine the two signals. To meet the target BER at the RN, the modulation order M_i of SN$_k$ should not be higher than 2^n, when $|h_k^u|^2\gamma < \gamma_{\text{PSK}}^{(n+1)}$, where h_k^u denotes the channel's coefficient spanning from SN$_k$ to RN. As a result, $M_i = 2^n$ for $\min\left\{\left(|h_i|^2 + |g_i|^2\right)\gamma, |h_k^u|^2\gamma\right\} \in \left[\gamma_{\text{PSK}}^{(n)}, \gamma_{\text{PSK}}^{(n+1)}\right)$.

Next, let us conceive adaptive NC-QAM from conventional adaptive QAM, which maps the transmitter's data to a symbol from 2^{2n}-ary QAM, [Here we focus on square QAM. The more general rectangular QAM scheme may be viewed as two parrel NC-PAM signals, which can be adapted individually.] when the receiver side SNR obeys $\gamma_{\text{QAM}} \in \left[\gamma_{\text{QAM}}^{(n)}, \gamma_{\text{QAM}}^{(n+1)}\right)$, where $\gamma_{\text{QAM}}^{(n)}, n = 0, 1, \ldots$ denotes the minimum SNR required for 2^{2n}-ary QAM to meet the target BER. [The specific value of $\gamma_{\text{QAM}}^{(n)}$ for $n < 4$ can be found in Table 1 of [27].] Note from (11) that NC-QAM has a SNR loss of λ_i. Hence, the modulation order M_i of the RN–DN$_i$ link can be chosen as $M_i = 2^{2n}$ for $\gamma_i = |h_i|^2\gamma \in \left[\lambda_i^{-1}\gamma_{\text{QAM}}^{(n)}, \lambda_i^{-1}\gamma_{\text{QAM}}^{(n+1)}\right)$. Since we have $\lambda_2 = 1$, the SNR threshold for the RN–DN$_2$ link is the same as that of the conventional adaptive QAM. Similarly, when NC-MRC is adopted, we have $M_i = 2^{2n}$ for $\min\left\{\left(\lambda_i|h_i|^2 + |g_i|^2\right)\gamma, |h_k^u|^2\gamma\right\} \in \left[\gamma_{\text{QAM}}^{(n)}, \gamma_{\text{QAM}}^{(n+1)}\right)$.

The adaptive NCM scheme may achieve a higher average throughput, which is presented by

$$\bar{R}_i = \sum_{n=1}^{N} n\left[F\left(\gamma_{\text{PSK}}^{(n+1)}\right) - F\left(\gamma_{\text{PSK}}^{(n)}\right)\right]$$

for adaptive NC-PSK and $\bar{R}_i = \sum_{n=1}^{N} 2n\left[F\left(\gamma_{\text{QAM}}^{(n+1)}\right) - F\left(\gamma_{\text{QAM}}^{(n)}\right)\right]$ for adaptive NC-QAM, where $F(x)$ denotes the cumulative distribution function (c.d.f.) of the equivalent receiver side SNR, which is, respectively, obtained by $|h_i|^2\gamma$ for NC-PSK, $\min\{(|h_i|^2 + |g_i|^2)\gamma, |h_k^u|^2\gamma\}$ for MRC-aided NC-PSK, $\lambda_i|h_i|^2\gamma$ for NC-QAM, and $\min\{(\lambda_i|h_i|^2 + |g_i|^2)\gamma, |h_k^u|^2\gamma\}$ for MRC-aided NC-QAM. More specifically, $F(x) = 1 - \mathrm{e}^{-\left(x/\overline{|h_i|^2}\gamma\right)}$ for NC-PSK and $F(x) = 1 - \mathrm{e}^{-\left(x/\lambda_i\overline{|h_i|^2}\gamma\right)}$ for NC-QAM. For MRC-aided NC-PSK and NC-QAM, we have

$$F(x) = \left(1 - \frac{\overline{|h_i|^2}\mathrm{e}^{-\left(x/\overline{|h_i|^2}\gamma\right)} - \overline{|g_i|^2}\mathrm{e}^{-\left(x/\overline{|g_i|^2}\gamma\right)}}{\overline{|g_i|^2} - \overline{|h_i|^2}}\right) \times \left(1 - \mathrm{e}^{-\left(x/\overline{|h_i^u|^2}\gamma\right)}\right)$$

and

$$F(x) = \left(1 - \frac{\lambda_i\overline{|h_i|^2}\mathrm{e}^{-\left(x/\lambda_i\overline{|h_i|^2}\gamma\right)} - \overline{|g_i|^2}\mathrm{e}^{-\left(x/\overline{|g_i|^2}\gamma\right)}}{\overline{|g_i|^2} - \lambda_i\overline{|h_i|^2}}\right) \times \left(1 - \mathrm{e}^{-\left(x/\overline{|h_i^u|^2}\gamma\right)}\right)$$

respectively, [$\overline{|h_i|^2} \neq \overline{|g_i|^2}$ and $\lambda_i\overline{|h_i|^2} \neq \overline{|g_i|^2}$ are assumed for NC-PSK and NC-QAM, respectively.]

5 Numerical results

In this section, a range of representative numerical results are presented for validating our theoretical analysis. Furthermore, NCM is compared with benchmark schemes for demonstrating its potential. Specifically, we invoke the so-called index-modulo based NC and analogue NC as benchmark schemes. The index-modulo-based NC maps the two messages intended for DN$_1$ and DN$_2$ to the symbol index $0 \le m_1 \le M_1 - 1$ and $0 \le m_2 \le M_2 - 1$. Then the output NC symbol is obtained by $X[m_1 + m_2 \text{mod} M_2]$. In analogue NC, RN broadcasts a symbol given by $X = \alpha\left(h_2^u X_1 + h_1^u X_2 + Z_R\right)$, which is an amplified version of the signal received from two concurrently transmitting SNs [In the following, we also assume the variance of the noise process Z_R at the RN receiver to be zero so as to formulate a SER lower bound of analogue NC. Let us assume that $|h_1^u| = |h_2^u| = 1$ for AWGN channels.].

Let us focus on the AWGN channels first, where it is assumed that $h_i = 1$ for $i = 1, 2$. Figs. 8 and 9 present the SER of NC-PSK where $M_1 = 2$ and $M_2 = 4$, and NC-QAM where $M_1 = 16$ and $M_2 = 64$, respectively. In both of figures, the theoretical and simulation results match well with each other. In particular, NC-PSK can achieve the same SER as if the RN transmitted exclusively to the single DN using PSK at the same bit rate and the same SNR, since having two receivers does not require an increased transmit power. This verifies the optimality of NCM for PSK constellations. As discussed in Section 4.1, NC-QAM may impose a modest SNR loss compared to classic one-way transmission at the receiver of DN$_1$. Quantitatively, for $M_1 = 16$, the SNR loss of DN$_1$ is < 0.21 dB, which is negligible in practice. In this figure, we also compared NC-PSK with the benchmark schemes to demonstrate its performance gain. In particular, NC-PSK is capable of achieving at least 3 dB SNR gain over the index-modulo-based NC at the RN–DN$_1$ link having lower data rate. NC-QAM achieves at least 5.7 dB SNR gain over the index-modulo-based NC at the RN–DN$_1$ link. These are both due to the fact that the minimum ED

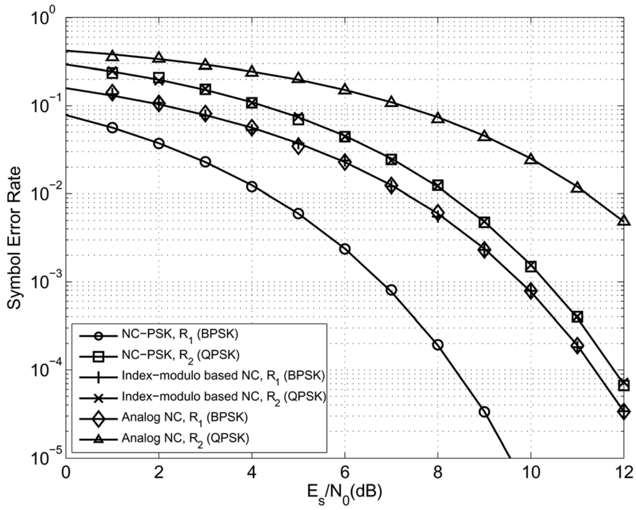

Fig. 8 *SER of NC-PSK, index-modulo-based NC and analogue NC, conditioned on $h_i = 1$*

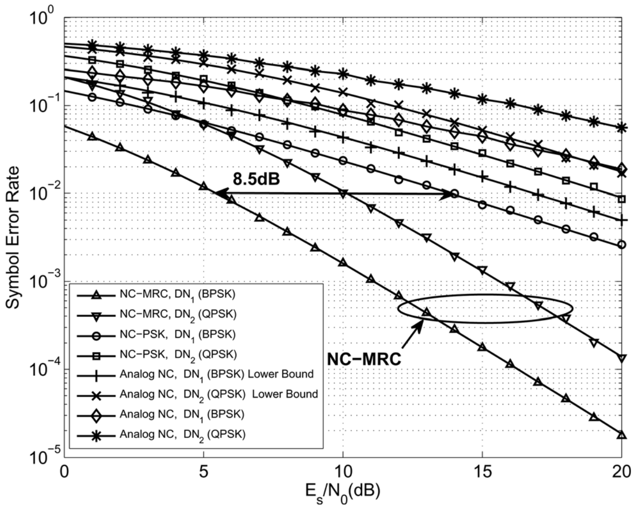

Fig. 10 *Average SER of NC-PSK with and without NC-MRC, index-modulo-based NC and analogue NC*

of legitimate symbols for DN_1 is maximised. Furthermore, both NC-SPK and NC-QAM achieve at least 3 dB SNR gain over analogue NC at the receivers of both DN_1 and DN_2 even though the uplink noise power at the RN's receiver is negligible. This is because the energy of symbol X is equally shared between X_1 and X_2 in analogue NC.

Next, let us turn our attention to fading channels, where we assumed that $|h_i|^2 = |g_i|^2 = 1$. Fig. 10 presents the average SER of NC-PSK both with and without NC-MRC. Again, the theoretical SER analysis is confirmed by the simulation results. Note that the slope of the average SER curves relying on NC-MRC is 2, whereas that without NC-MRC is only 1. This figure also shows that the benchmark scheme, for example, the analogue NC [For Rayleigh channels, the lower bound is formulated by assuming the variance of the noise process Z_R at the RN receiver to be zero and $|h_1^u| = |h_2^u| = 1$.] relying on PSK achieves a diversity order of 1. Thus, it can be concluded that NC-MRC is capable of attaining a beneficial diversity gain of 2 for NC-PSK. It is worth noting that although NC-MRC is beneficial, it cannot be invoked in two-timeslot-based NC schemes, where SN_1 and SN_2 transmit simultaneously during the first timeslot. Owing to the ubiqitous half-duplex constraint, DN_1 and DN_2 are unable to directly receive any signal from each other. As a result, the diversity order of two-timeslot-based NC schemes is essentially bounded by 1. In other words, although two-timeslot NC schemes achieve a spectral efficiency gain of 33% over our three-timeslot NC scheme, they suffer from a poorer reliability than MRC aided NCM. Furthermore, because of its higher diversity gain, NC-MRC aided NC-PSK is also capable of achieving a significant SNR gain over two-timeslot NC schemes using PSK constellations in the high-SNR, that is, low-SER region. Quantitatively, at the average SER of 10^{-2}, NC-MRC achieves at least 8.5 dB SNR gain over TWR operating without NC-MRC, such as analogue NC using PSK constellations.

Finally, the average SER of NC-QAM operating both with and without NC-MRC is presented in Fig. 11, where the theoretical and numerical results match well with each other. Observe that NC-MRC achieves a diversity gain of 2 over other QAM-based TWR operating without MRC, such as analogue NC using QAM constellations. This beneficial diversity gain results in a substantial SNR-gain of 9.7 dB,

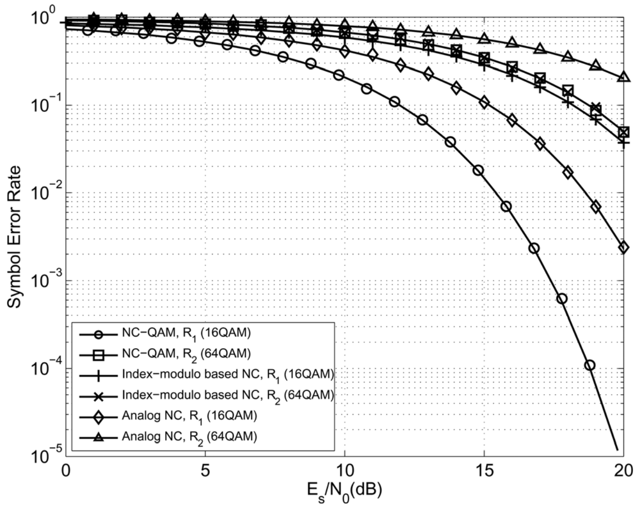

Fig. 9 *SER of NC-QAM, Index-modulo-based NC and analogue NC, conditioned on $h_i = 1$*

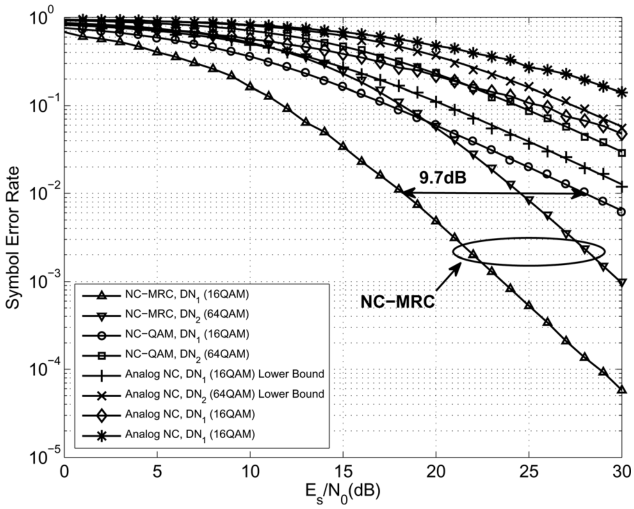

Fig. 11 *Average SER of NC-QAM with and without NC-MRC, index-modulo-based NC, and analogue NC*

doi: 10.1049/iet-com.2012.0819

as shown in Fig. 11. In conclusion, NCM achieves a significant SNR gain over the index-modulo-based NC and analogue NC schemes having the same constellations in AWGN channels, whereas NC-MRC, which can only be applied in three-timeslot based NC, is capable of achieving both a significant diversity gain and an SNR gain over the two-timeslot benchmark NC, that is, the analogue NC in Rayleigh fading channels.

6 Conclusions and future research

In this paper, practical NCM schemes were proposed for asymmetric DF-TWR, where the symbol rate of two traffic flows can be different. For arbitrary constellation, we proposed a set-partitioning technique for universal NCM, which maximises the ED of legitimate symbols for both receivers. More practically, based on the modulo addition of the normalised symbol phase/amplitude, we conceived NC-PSK/QAM, which is based on the appropriately rotated or circularly-shifted classic PSK/QAM symbols. This relationship allows us to borrow the SER analysis method of classic PSK/QAM for deriving the SER of NC-PSK/QAM. NC-PSK is capable of achieving a SER at both receivers, as if the RN transmitted exclusively to a single receiver only. Based on the relationship between NC-PSK/QAM and classic PSK/QAM, a new MRC was proposed for combining the NC signal received from the RN and the original signal overheard from the SN at the DN. The NC-MRC scheme is capable of achieving the maximum cooperative diversity gain of 2 by exploiting the pair of independently fading paths from the SN and RN, thereby achieving a substantial performance gain over the TWR operating without MRC. Furthermore, the adaptive NCM is also proposed in order to maximise the throughput of both time-varying $RN-DN_1$ and $RN-DN_2$ links, whereas guaranteeing a target BER. As to future research, it is possible to extend NCM for it to become compatible with existing physical layer techniques such as channel coding. Another important future direction is to extend the methodology of NCM to analogue NC using only two-timeslot per transmission.

7 Acknowledgment

The authors would like to thank the associate editor and anonymous reviewers for their careful reading and constructive comments. L. Hanzo would also like to thank the Euroepan Research Council (ERC) for their fiscal support under the Advance Fellow Grant.

8 References

1 Ahlswede, R., Cai, N., Li, S.-Y.R., Yeung, R.W.: 'Network information flow', *IEEE Trans. Inf. Theory*, 2000, **46**, pp. 1204–1214
2 Li, S.-Y.R., Yeung, R.W., Cai, N.: 'Linear network coding', *IEEE Trans. Inf. Theory*, 2003, **49**, pp. 371–381
3 Koetter, R., Medard, M.: 'An algebraic approach to network coding', *IEEE/ACM Trans. Netw.*, 2003, **11**, pp. 782–795
4 Wu, Y., Chou, P.A., Kung, S.-Y.: 'Information exchange in wireless networks with network coding and physical-layer broadcast'. Microsoft Research, Technical Report, MSR-TR -2004-78, August 2004
5 Katti, S., Rahul, H., Hu, W., Katabi, D., Medard, M., Crowcroft, J.: 'XORs in the air: practical wireless network coding', *IEEE/ACM Trans. Netw.*, 2008, **16**, pp. 497–510
6 Zhang, S.L., Liew, S.C., Lam, P.P.: 'Physical-layer network coding'. Proc. ACM Mobicom, Los Angeles, USA, September 2006
7 Popovski, P., Yomo, H.: 'Wireless network coding by amplify-and-forward for bi-directional traffic flows', *IEEE Commun. Lett.*, 2007, **11**, pp. 16–18
8 Koike-Akino, T., Popovski, P., Tarokh, V.: 'Optimized constellations for two-way wireless relaying with physical network coding', *IEEE J. Sel. Areas Commun.*, 2009, **27**, pp. 773–787
9 Xie, L.-L.: 'Network coding and random binning for multi-user channels'. Proc. 10th Canadian Workshop on Information Theory, Alberta, June 2007, pp. 85–88
10 Wu, Y.: 'Broadcasting when receivers know some messages a priori'. Proc. IEEE Int. Symp. on Information Theory, Nice, France, June 2007, pp. 1141–1145
11 Chen, W., Letaief, K.B., Cao, Z.: 'A cross-layer method for interference cancellation and network coding in wireless networks'. Proc. IEEE Int. Conf. Communications, Istanbul, Turkey, June 2006, pp. 3693–3698
12 Narayanan, K., Wilson, M.P., Sprintson, A.: 'Joint physical layer coding and network coding for bi-directional relaying'. Proc. Allerton Conf. Communication, Control and Computing, Monticello, IL, USA, August 2007
13 Baik, I.-J., Chung, S.-Y.: 'Network coding for two-way relay channels using lattices'. Proc. IEEE Int. Conf. Communications, Beijing, China, May 2008, pp. 3898–3902
14 Kim, R.Y., Kim, Y.Y.: 'Symbol-level random network coded cooperation with hierarchical modulation in relay communication', *IEEE Trans. Consum. Electron.*, 2009, **55**, pp. 1280–1285
15 Sykora, J., Burr, A.: 'Network coded modulation with partial side-information and hierarchical decode and forward relay sharing in multi-source wireless network'. Proc. European Wireless Conf., Tuscany, Italy, April 2010, pp. 639–645
16 Chen, W., Hanzo, L., Cao, Z.: 'Network coded modulation for two-way relaying'. Proc. IEEE WCNC, Cancun, Mexico, March 2011
17 Park, J.M., Kim, S.-L., Choi, J.: 'Hierarchically modulated network coding for asymmetric two-way relay systems', *IEEE Trans. Veh. Technol.*, 2010, **59**, pp. 2179–2184
18 Sykora, J., Jorswieck, E.A.: 'Network coded modulation with HDF strategy and optimized beam-forming in 2-source 2-relay network'. Proc. IEEE VTC, San Francisco, USA, September 2011
19 Li, X., Jiang, T., Zhang, Q., Wang, L.: 'Binary linear multicast network coding on acyclic networks: principles and applications in wireless communication networks', *IEEE J. Sel. Areas Commun.*, 2009, **27**, (5), pp. 738–748
20 Chen, Z., Liu, H., Wang, W.: 'A novel decoding-and-forward scheme with joint modulation for two-way relay channel', *IEEE Commun. Lett.*, 2010, **14**, (12), pp. 1149–1151
21 Cao, R.H., Lv, T.J., Gao, H.: 'Symbol-based physical-layer network coding for two-way relay channel'. Proceedings of MILCOM 2011, 7–10 Nov. 2011, pp. 287–292
22 Ungerboeck, G.: 'Trellis-coded modulation with redundant signal sets', *IEEE Commun. Mag.*, 1987, **25**, pp. 5–21
23 Hanzo, L., *et al.*: 'Quadrature amplitude modulation: from basics to adaptive trellis-coded, turbo-equalised and space-time coded OFDM, CDMA and MC-CDMA systems' (Wiley-IEEE Press, 2004, 2nd edn.) **Q3**
24 Proakis, J.G.: 'Digital communications' (McGraw-Hill, New York, 2007, 5th edn.)
25 Simon, M.K., Alouni, M.-S.: 'Digital communications over fading channels' (John Wiley & Sons, New York, 2005, 2nd edn.)
26 Chung, S.T., Goldsmith, A.J.: 'Degrees of freedom in adaptive modulation: a unified view', *IEEE Trans. Commun.*, 2001, **49**, (9), pp. 1561–1571
27 Liu, Q., Zhou, S., Giannakis, G.B.: 'Cross-layer combining of adaptive modulation and coding with truncated ARQ over wireless links', *IEEE Trans. Wirel. Commun.*, 2004, **3**, (5), pp. 1746–1755

www.ietdl.org

COM20120819

Author Queries

Wei Chen, Zhigang Cao, Lajos Hanzo

Q1 Please expand BEP and XOR.

Q2 All footnotes have been moved to text as required by journal style. Please check and confirm that they have been located correctly within the text.

Q3 As per journal style, names of up to six authors are provided. If there are more than six, only the first three should be given followed by et al. Please provide next …… author names in Refs. [23] as required by journal style.